Microscopic damage size in fiber-reinforced polymer-matrix composites: quantification approac via NDT-measurements

Andreas J. Brunner, Philipp Potstada, Markus G. R. Sause

Angaben zur Veröffentlichung / Publication details:

Brunner, Andreas J., Philipp Potstada, and Markus G. R. Sause. 2019. "Microscopic damage size in fiber-reinforced polymer-matrix composites: quantification approac via NDT-measurements." *Procedia Structural Integrity* 17: 146–53. https://doi.org/10.1016/j.prostr.2019.08.020.

Available online at www.sciencedirect.com

ScienceDirect

Procedia Structural Integrity 17 (2019) 146–153

Structural Integrity Procedia

www.elsevier.com/locate/procedia

ICSI 2019 The 3rd International Conference on Structural Integrity

Microscopic damage size in fiber-reinforced polymer-matrix composites: Quantification approach via NDT-measurements

Andreas J. Brunner[a]*, Philipp Potstada[b], Markus G.R. Sause[b]

[a]*Empa, Swiss Federal Laboratories for Materials Science and Technology, Laboratory for Mechanical Systems Engineering, Ueberlandstrasse 129, CH-8600 Duebendorf, Switzerland*

[b]*University of Augsburg, Institute for Materials Resource Management, Universitätsstr. 1 Nord, D-86159 Augsburg, Germany*

Abstract

The meso-scale morphology of fiber-reinforced polymer-matrix (FRP) composites with fiber plies induces a range of microscopic damage mechanisms when FRP materials are subject to mechanical or thermo-mechanical loading. Both, for improving the damage resistance of FRP composites and for structural design guidelines, understanding the different damage mechanisms and their interaction is important. Acoustic Emission (AE) monitoring of load tests on laboratory-scale FRP specimens yields information on the occurrence of damage as a function of stress level, and typically allows for roughly locating signal sources, and with sophisticated pattern recognition, for identification of different micro- or mesoscopic damage mechanisms. In FRP components and elements empirical criteria for assessing structural integrity, e.g., AE Felicity-ratio, yield quantitative failure predictions. Combining AE information on microscopic damage mechanisms with macroscopic, empirical criteria has not received much attention yet. Identifying which mechanisms, e.g., damage from stress-relaxation or friction of existing crack faces induces the onset of AE signals in FRP composites and thus defines the Felicity-ratio is important for structural integrity characterization. This approach to the Felicity effect on the microscopic scale and its advantages and limitations are presented and discussed.

Peer-review under responsibility of the ICSI 2019 organizers.

Keywords: Fiber-reinforced polymer composites; Acoustic emission; Felicity effect; Quantificaiton of damage; Microscopic damage mechanisms; Non-destructive test

* Corresponding author. Tel.: +41-58-765-4493; fax: : +41-58-765-6911.
E-mail address: andreas.brunner@empa.ch

2452-3216
Peer-review under responsibility of the ICSI 2019 organizers.
10.1016/j.prostr.2019.08.020

1. Introduction

Assessing the structural integrity or the remaining service life-time of FRP composite load-bearing elements or pressure vessels is often difficult due to several factors. Among them are the complex, multi-scale morphology of FRP composites which induces a range of different microscopic and mesoscopic damage mechanisms; the interaction between often multi-axial external loads with residual stresses and defects from manufacturing and processing; and the comparatively high sensitivity of FRP composites to environmental exposure, e.g., temperature and humidity variations. Mechanical properties of interest for these materials are tensile strength and stiffness (specific strength and stiffness are relatively high due to their rather low specific density), whereas their susceptibility to impact damage, e.g., formation of matrix cracks or delaminations, shear failure between fiber plies inside the laminates, and relatively brittle failure (especially for thermoset matrix polymers) are weak points. For a long time, structural integrity assessment of FRP parts or components using AE monitoring of load tests was mainly based on empirical criteria for damage initiation and accumulation. This was due to the mechanisms creating the AE signals (essentially elastic waves from energy release propagating in the materials), i.e., microscopic damage events on scales of a few hundred micrometers or less, such as micro-crack formation in the matrix, fiber-matrix debonding or fiber failure. Hence it was, until recently, difficult to identify the mechanisms and locate the sources of these unambiguously or with sufficient confidence in order to develop and apply damage models for service life predictions.

Nomenclature

AE	Acoustic emission
ASTM	American Society for Testing and Materials, International
CFRP	Carbon fiber-reinforced polymer
DCB	Double cantilever beam (specimen)
FR	Felicity-ratio
FRP	Fiber-reinforced polymer
FFT	Fast Fourier transform
NDT	Non-destructive test
PEEK	Poly-ether-ether-ketone
RVE	Representative volume element
SR-μCT	Synchrotron radiation X-ray computed micro-tomography
X-ray CT	X-ray computed tomography
X-ray μCT	X-ray computed micro-tomography
2D	two-dimensional

The Felicity effect in AE yields a quantitative indicator in the form of the FR for damage accumulation in FRP composite materials and components. Essentially, the effect is the occurrence or observation of AE at load levels below the earlier maximum load or stress level when the test object is reloaded from a lower load again. In AE terminology standards, i.e., ASTM E1316 (2018), EN 1330-9 (2017), and ISO 12716 (2001), the term FR is defined with slight differences in the specification of certain details. For the quantification of the FR, the ratio between the load level at which AE is observed upon reloading divided by the previous maximum load level, i.e., a value lower than 1, the following qualifications are essential. However, not all of these are explicitly noted in the standards. The first is that the recording of AE throughout both load steps uses the same sensitivity level (implying same signal acquisition threshold, same sensor and measurement chain characteristics and constant sensor coupling to the test object). This is specified only in ASTM E1316 (2018), but not in other standards. The second qualification is that the AE indicating the load in the second load step for calculating the FR is "significant" as stated in EN 1330-9 (2017). This standard then simply notes that what constitutes "significant" depends on the application, whereas ASTM E1067/1076M (2018) gives some guidance on that in terms of possible AE activity and AE intensity criteria where number of emissions and their duration, respectively, are used. The third qualification, not stated in any standard (possibly assumed to be a trivial one) is that the AE is caused by damage initiation or propagation in the test object and not by external factors,

such as noise from the environment, e.g., spurious signals caused in the loading device, e.g., by friction, or in the piezoelectric sensor material due to temperature fluctuations or electromagnetic interference. From this perspective, it is evident that the confidence with which the FR can be determined could be improved if the source mechanisms of all AE signals recorded during the tests are identified unambiguously or with sufficient probability. Thus, noise and other non-relevant signals could be discriminated and eliminated in the FR analysis. Further, if in addition to the identification of the underlying mechanisms, the AE signal sources could be located with sufficient accuracy, clustering of signal sources would indicate where a transition from distributed defect formation or damage to accumulation of localized damage growth is taking place. This, combined with the knowledge of the respective damage mechanism(s), might indicate possible failure location(s) and expected failure mode(s) directly, or could be used as input for detailed damage mechanics models for quantitatively predicting service life-time and the expected failure mode(s). Furthermore, using an artificial neural network, an evaluation of the FR values also provides a tool to predict the material failure stress as discussed by Sause et al. (2018).

Recent advances in AE analysis using unsupervised pattern recognition for identifying AE signal classes likely correlating with different source mechanisms are discussed in detail by Sause (2016). Neural networks, artificial intelligence and related algorithms for accurately determining AE signal source locations even in anisotropic materials are described, e.g., by Ono (2018) or Das et al. (2019). The combination of identifying the damage mechanisms and locating the damage by AE seems promising for achieving improved, i.e., more accurate and reliable FR values for predicting failure loads and failure locations for FRP composite components and structures. The unambiguous identification of the damage mechanisms represented by the different clusters from unsupervised AE signal pattern recognition requires either independent information from NDT, e.g., X-ray μCT imaging as shown by Baensch et al. (2015) and Potstada et al. (2018), or detailed physics-based simulations taking into account localized source mechanisms, signal propagation effects, and signal modification by the sensor and measurement chain characteristics as discussed by Sause (2016).

The present contribution hence explores the feasibility and current limitations of the FR evaluation. Selected examples of combined AE monitoring and in-situ NDT of selected load-tests on FRP composite test coupons or test objects are discussed, highlighting the current state of the art as well as identifying needs for additional research in order to achieve better predictions of failure loads, failure locations or failure modes of FRP components and structures.

2. Materials and Methods

The examples discussed in this paper are dealing with CFRP composite laminates with essentially continuous carbon fibers embedded in a thermoplastic or in a thermoset matrix polymer. Details of the test specimens or test objects discussed here are given in the literature referenced in the results section below.

AE measurements are performed with piezo-ceramic sensors and dedicated equipment, the recorded AE signals are analyzed either by the equipment specific software or special software developed by the authors.

The method chosen here for getting complementary information for interpreting the AE data is in-situ SR μCT, see, e.g., Wu et al. (2017), or X-ray μCT, the experimental details for the former are given by Potstada et al. (2018).

3. Selected Examples and Discussion

In composite structures, AE monitoring of load tests can give "early" indications of the failure load and possibly also of the location of failure. For the first question, i.e., failure load prediction, FR analysis has been shown to give quantitative, reliable results, for example for different types of balsa-wood-CFRP T-joints under tensile or compressive loading as discussed by Brunner and Paradies (2000). Fig. 1 shows the FR-values and an extrapolation from a part of the FR-data, respectively, determined from AE activity recorded during a step-wise tensile load test on one type of T-joint. Fig. 2 shows examples of the AE activity (number of signals per unit time) recorded during the test with resonant AE sensors (type SE150-M with 150 kHz resonant frequency). The comparison between the FR-values determined from AE activity recorded by individual sensors shows some scatter between sensors in different locations, as well as with that of the overall recorded AE activity (i.e., from all sensors used). It is interesting to note that the overall activity provides a lower bound in this plot that could be used as a "conservative" estimate. An AE

activity criterion of at least five hits per second has been taken as indication of "significant" AE and used together with the nominal load of the previous load level for the calculation of all FR-values. The types of mechanism producing these AE signals could not be identified, since only AE signal parameters but not full AE waveforms required for pattern recognition had been recorded in these tests. If a FR-value of 0.95 is taken to be critical, the single sensor data only reach or go below this critical limit for the last load step (from 90 kN up to 100 kN). The overall AE activity, on the other hand, yields this limit already when reloading from the seventh load step, from 70 kN up to 80 kN, i.e., at a 20-30% margin below the quasi-static failure load of about 100 kN.

An extrapolation of the first five FR-values determined from the overall AE activity (up to a load of 50 kN which can be considered a maximum service load) yields essentially the same result, i.e., a critical value of 0.95 for loads around about 75 kN. Of course, this simple empirical estimate of critical stress or load can be improved by testing a larger number of nominally identical objects and building a data base. In addition to improving quantitative failure load predictions, the scatter in the data could also be estimated (e.g., a 95% confidence interval). Analyzing additional criteria, i.e., AE activity (e.g., specified number of AE signals per margin of load increase or during load hold) or AE intensity (e.g., AE signal duration per margin of load increase or AE amplitude) discussed in ASTM E1067/1067-M (2018) contribute to further improvement of the quality of the prediction. The failure location may be predicted from AE activity or AE intensity, i.e., identifying the sensor or sensor array yielding the highest cumulative number of AE signals or of AE signal amplitude or energy, respectively, Fig. 2 shows, however, that the AE activity (measured in number of AE signals recorded per second) reaches peak values in the early load steps (second to fourth load step), and then decreases with increasing load levels, Whether this reflects a real reduction in the amount of damage created in higher load steps or is due to AE signal attenuation by damage accumulation and propagation is not clear.

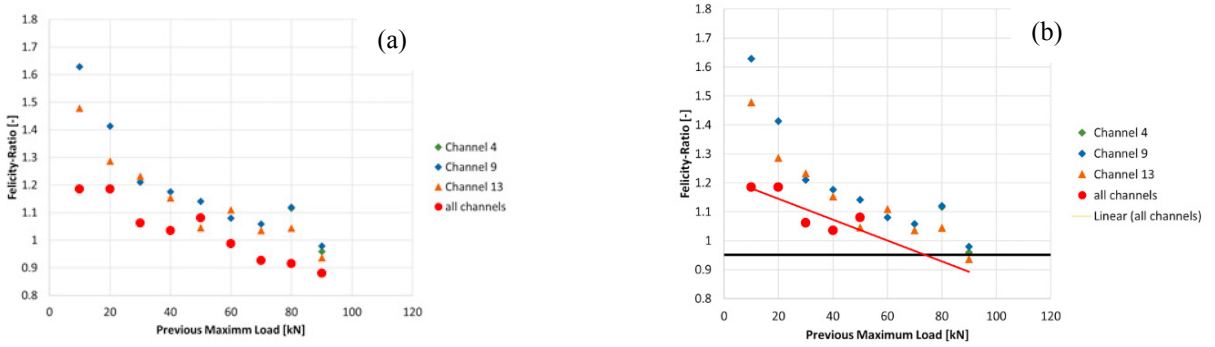

Fig. 1. (a) Felicity-ratio (FR) as a function of load steps; (b) Extrapolation of FR as a function of load steps.

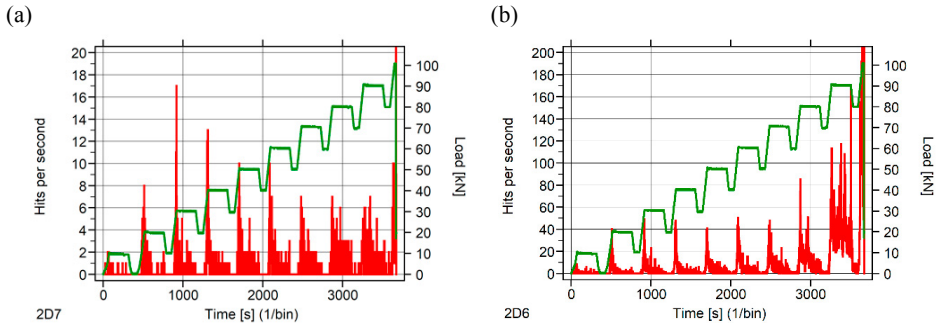

Fig. 2. (a) AE activity of one sensor (b) AE activity of all sensors (red curves) and load levels (green curves), both as a function time; note the difference in scale.

The duration of AE activity at nominally constant load (the tests were performed under displacement control, i.e., there was a small amount of load relaxation at constant displacement), however, is increasing with increasing number of load steps and persists for up to four minutes at loads above 50 kN. According to ASTM 1067/1067-M this clearly supports the interpretation of the FR-values that significant damage is created with increasing load levels. The type of

damage mechanism producing the recorded AE signals, as noted above, has not been considered in this approach. Depending on the test set-up, AE signals could also come from other sources, e.g., friction between load frame and test object or between internal defect surfaces that do not relate to the damage accumulation. Such noise signals could affect the FR-values and lead to predictions overestimating the damage and hence underestimating the failure load. Accordingly, noise signals not related to damage accumulation in the test objects should be excluded. One approach for filtering noise signals coming from sources not related to damage initiation or propagation in the material is the use of so-called "guard"-sensors placed, for example, on the load introduction(s), and all AE signals arriving at those sensors first are disregarded. However, this approach may not eliminate all noise signals such as signals from friction between crack surfaces. These indicate the presence of existing defects, but are not necessarily showing defect propagation or increasing damage. Hence, the feasibility of identifying microscopic source mechanisms of AE signals for a more reliable FR value determination will be discussed here. AE signal source location based on arrival times of the AE signals is usually limited to centimeter accuracy in typical laboratory-scale FRP parts or components, and to a few centimeters for larger scale FRP parts, if artificial neural networks are used as shown by Kalafat and Sause (2015).

Small-scale CFRP specimen with edge length of < 2 mm are well suited to study in-situ with SR µCT. Due to the high resolution of state-of-the-art scanner systems, this allows to study the generation of microscopic damage and to compare it to the simultaneously recorded AE signals. Fig. 3(a) shows an example of an experimental setup for an in-situ SR µCT in combination with AE monitoring. Based on high spatial resolution (<500 nm) and high beam fidelity, the resulting images allow virtual cross-sections, that allow identifying the initiation and growth of cracks in Fig. 3(b). For the in-situ load experiments, the sample is loaded with step-wise increased load, so the cracks stay open. This even allows to track the growth and accumulation of fiber breaks, see, e.g., Wright et al. (2010) or Garcea et al. (2014). In Potstada et al. (2018) this has been recently used to verify the signature of AE signals caused by fiber breaks. However, it remains speculative, whether the analysis of such small volumes is sufficient to reveal the origin of the AE signals for calculating improved FR values.

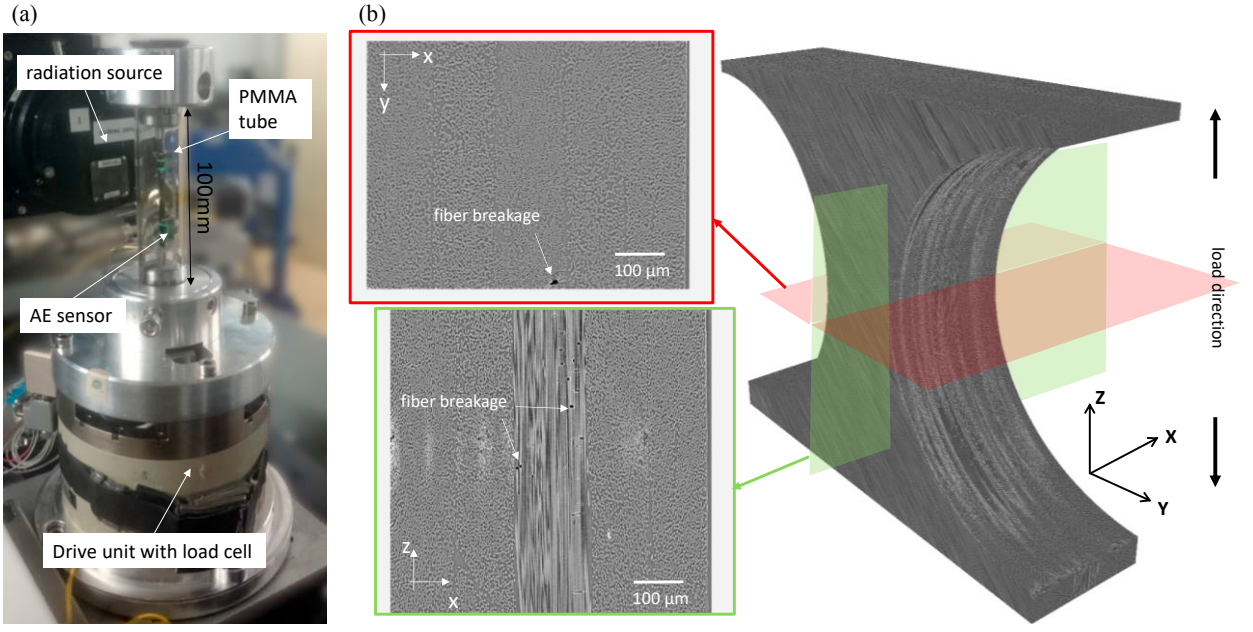

Fig. 3. (a) Setup for X-ray µCT with simultaneous AE monitoring; (b) Example for scanned volume at notch position with two virtual cross-sections to identify particular damage types.

In general, the same approach can also be applied to laboratory-scale test coupons on the laminate scale (cross-section 10 mm – 20 mm × thickness). However, for X-ray CT, the resolution of the images depends on the specimen size, microscopic resolution in the micrometer or sub-micrometer range (e.g., defined by voxel size) usually requires specimens not larger than centimeter size. Hence, the resolution is expected to decrease for typical laminate scale

samples. In Fig. 4(a) a custom-made 20 kN in-situ load stage usable for commercial computed tomography devices is shown. The typical specimen size in Fig. 4(b) allows covering the dimensions of a laminate architecture and still provides sufficient imaging quality to track the initiation and growth of cracks. Fig. 4(c) shows a comparison of the volume at 10 kN load and at 13 kN load. In the virtual xz-cross-section the formation of cracks in the off-axis plies is easy to identify and to track. Such a setting allows to study the interaction between plies and might prove as the right tool to reveal the origin of the FR. For large-scale components, e.g., even up to the size of trucks or railway cargo cars, there are high-energy X-ray imaging scanning systems available, see, e.g., Kolokytha et al. (2018). Such systems, in principle, could be implemented for in-situ monitoring of load tests on large (meter size and higher) FRP components and structures. However, the image resolution (of millimetre to centimetre scale, essentially depending on the type of detector and the set-up of the test) would not allow for identifying the type of microscopic damage that is associated with the release of AE signals.

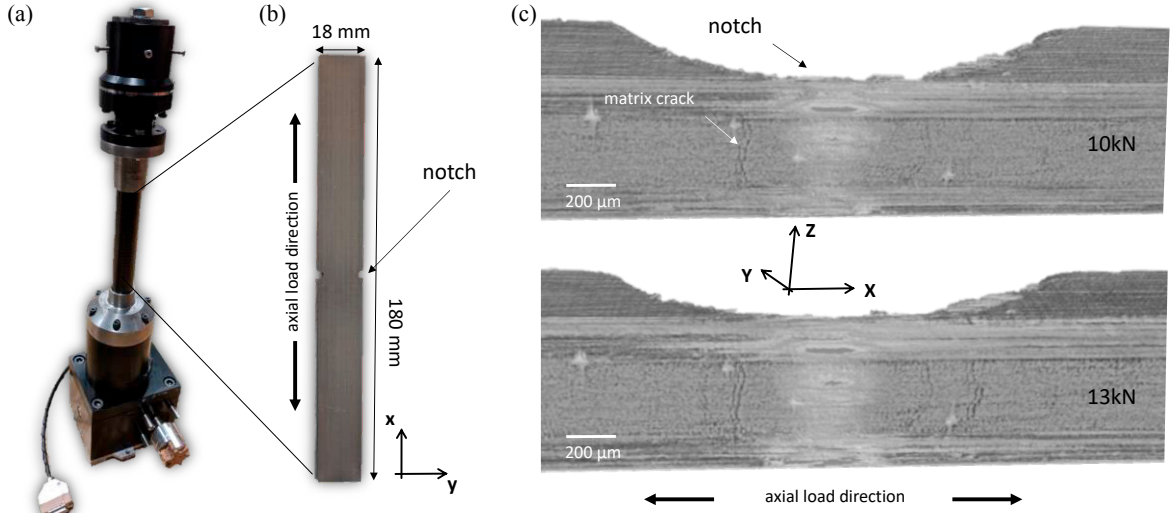

Fig. 4. (a) Loading device for in-situ X-ray computed micro-tomography; (b) the notched tensile CFRP specimen geometry and size; (c) selected tomography slices from the notch area of the specimen.

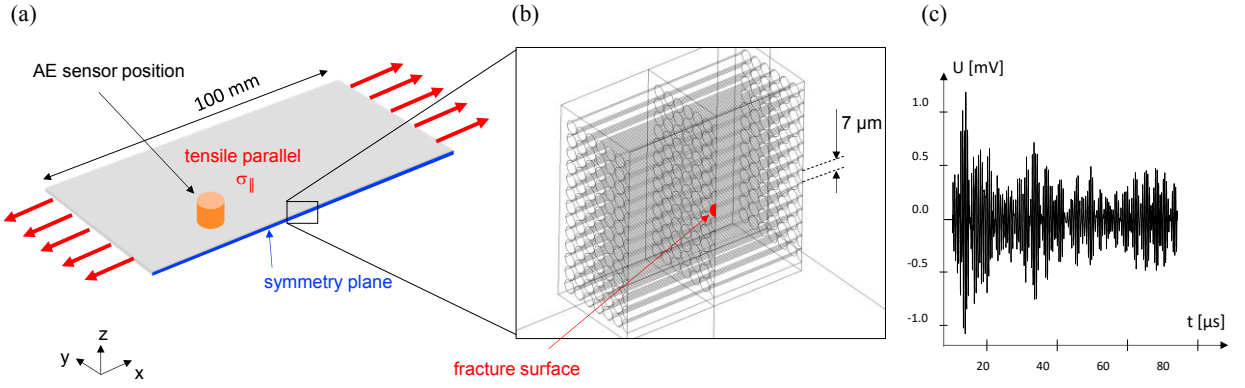

Fig. 5. (a) Modelling setup for unidirectional laminate subject to tensile load; (b) Zoom to embedded RVE with model of single fiber breakage; (c) resulting modeled AE signal for fiber breakage of single filament detected at 50 mm distance to the source.

As an alternative, modelling can contribute to the identification of the microscopic mechanisms producing the AE signals during load testing of FRP specimens. Such finite element models allow to simulate the AE signals by implementing model damage sources in FRP materials and to consider the effects of signal wave propagation in the anisotropic FRP materials and the specimen geometry, as well as the effects of the sensor characteristic (sensitivity as a function of frequency), see e.g. Sause (2016). In this context in-situ SR µCT experiments, allow the proper validation

of AE source models, since the origin of the AE signal can be directly identified and then modeled using finite elements. For larger objects a multi-scale approach was developed that uses an embedded RVE on the inside of a stressed body (see Fig. 5(a) and 5(b)), see e.g. Sause (2016) for details. The flexibility of such modeling approaches then allows studying effects of wave propagation and can provide an estimate of the expected AE signal characteristics for a particular failure type at a given location.

4. Summary and Outlook

The selected examples illustrate how AE from testing various FRP specimens or components combined with in-situ X-ray computed micro-tomography can contribute to the identification of the microscopic damage mechanisms and the determination of their location. The location accuracy, however, is limited for X-ray imaging by the spatial resolution depending on the test object size and the X-ray source and detector system used. For large test objects, this may become comparable the roughly centimeter size accuracy of the signal source location that can be achieved by AE. Complementary information from X-ray computed tomography or from finite element simulations can contribute to either improving the failure load or service-life predictions derived from AE monitoring using empirical criteria, e.g., the FR-values, or for development of damage models. The origin, and hence, reliability of this value is currently assessed with high-resolution in-situ imaging from X-ray CT or X-ray μCT up to laboratory scale. The simultaneous monitoring with AE provides a basis for the identification of mechanisms from AE signal analysis using unsupervised pattern recognition and complementary information from NDT or modelling. The question remains whether AE sources not related to damage initiation or accumulation, such as friction, affect the AE data to an extent, that the determination of the FR-value on the structural scale becomes highly unreliable.

Acknowledgements

The assistance of Rolf Paradies for the performance and analysis of the mechanical data of the T-joint tests and of Daniel Völki for the test setup are gratefully acknowledged. The contributions of Ian Sinclair and Sebastian Rosini for their skilled support in the in-situ experiments are also acknowledged.

References

ASTM E1067/1076M, (2018). Standard Practice for Acoustic Emission Examination of Fiberglass Reinforced Plastic Resin (FRP) Tanks/Vessels, American Society for Testing and Materials, International, 1-16.

ASTM E1316, (2018). Standard Terminology for Nondestructive Examinations, American Society for Testing and Materials, International, 1-39.

Baensch, F., Zauner, M., Sanabria, S.J., Pinzer, B.R., Sause, M.G.R., Brunner, A.J., Stampanoni, M., Niemz, P., (2015). Damage Evolution in Wood – Synchrotron based microtomography (SRμCT) as complementary evidence for interpreting acoustic emission behavior“, Holzforschung 68(8) 1015-1025.

Brunner, A.J., Paradies, R., (2000). Comparison of Designs of CFRP-Sandwich T-Joints for Surface Effect Ships Based on Acoustic Emission Analysis from Load Tests, in: Composite Structures: Theory and Practice, ASTM Special Technical Publication STP 1383 (Eds. P. Grant, C.Q. Rousseau), American Society for Testing and Materials, 366-381.

Das, A.K., Lai T.T., Chan C.W., Leung C.K.Y, (2019). A new non-linear framework for localization of acoustic sources Structural Health Monitoring 18(2) 590–601.

EN 1330-9, (2017). Non-destructive testing - Terminology - Part 9: Terms used in acoustic emission testing, Comité Européen de Normalisation, 1-13.

Garcea S.C., Mavrogordato M.N., Scott A.E:, Sinclair I., Spearing S.M., (2014) Fatigue micromechanism characterisation in carbon fibre reinforced polymers using synchrotron radiation computed tomography, Composites Science and Technology 99 23–30.

ISO 12716, (2001). Non-destructive testing — Acoustic emission inspection — Vocabulary, International Organization for Standardization, 1-11.

Kolokytha, S., Flisch, A., Lüthi, Th., Plamondon, M., Visser, W., Schwaninger, A., et al. (2017) Creating a reference database of cargo inspection X-ray images using high energy radiographs of cargo mock-ups, Multimedia Tools and Applications 77 9379–9391.

Ono, K., (2018). Review on Structural Health Evaluation with Acoustic Emission, Applied Science, 8 958, 1-33.

Potstada P., Rosini S., Mayrogordato M. Sinclair, I., Spearing S.M., Sause, M.G.R., (2018). Combination of Synchrotron Computed Tomography and Acoustic Emission Measurements for Cyclic Loading of Fibre-Reinforced Composites, Proceedings 33rd European Conference on Acoustic Emission Testing, Paper No. 04, 1-11.

Sause, M. G. R. (2016). Acoustic Emission. In Springer Series in Materials Science, Vol. 242, pp. 131–359.

Sause M.G.R., Schmitt S., Kalafat S., (2018). Failure load prediction for fiber-reinforced composites based on acoustic emission, Composites Science and Technology 164 24–33.

Wright P., Moffat A., Sinclair I., Spearing S.M., (2010) High resolution tomographic imaging and modelling of notch tip damage in a laminated composite, Composites Science and Technology 70 1444–1452.

Wu, S.C., Xiao, T.Q., Withers, P.J. (2017). The imaging of failure in structural materials by synchrotron radiation X-ray microtomography, Engineering Fracture Mechanics 182 127–156.